Editors' Suggestion   Featured in Physics

Model Construction and a Possibility of Cupratelike Pairing in a New d^9 Nickelate Superconductor (Nd,Sr)NiO$_2$

Hirofumi Sakakibara[1,2,3,*] Hidetomo Usui,[4] Katsuhiro Suzuki,[5] Takao Kotani,[1] Hideo Aoki,[6,7] and Kazuhiko Kuroki[8]

[1]Department of Applied Mathematics and Physics, Tottori University, Tottori, Tottori 680-8552, Japan
[2]Advanced Mechanical and Electronic System Research Center(AMES), Tottori University, Tottori, Tottori 680-8552, Japan
[3]Computational Condensed Matter Physics Laboratory, RIKEN Cluster for Pioneering Research (CPR),
Wako, Saitama 351-0198, Japan
[4]Department of Physics and Materials Science, Shimane University, Matsue, Shimane 690-8504, Japan
[5]Division of Materials and Manufacturing Science, Graduate School of Engineering, Osaka University, Suita, Osaka 565-0871, Japan
[6]National Institute of Advanced Industrial Science and Technology (AIST), Tsukuba, Ibaraki 305-8568, Japan
[7]Department of Physics, The University of Tokyo, Hongo, Tokyo 113-0033, Japan
[8]Department of Physics, Osaka University, Toyonaka, Osaka 560-0043, Japan

Effective models are constructed for a newly discovered superconductor (Nd, Sr)NiO$_2$, which has been considered as a possible nickelate analog of the cuprates. Estimation of the effective interaction, which turns out to require a multiorbital model that takes account of all the orbitals involved on the Fermi surface, shows that the effective interactions are significantly larger than in the cuprates. A fluctuation exchange study suggests occurrence of $d_{x^2-y^2}$-wave superconductivity, where the transition temperature should be lowered from the cuprates due to the larger interaction.

Introduction.—While it has been more than three decades since high-T_c superconductivity was discovered in the cuprates, search for their analogs in noncopper-based materials has remained a big challenge, both experimentally and theoretically. In particular, nickelates have attracted attention due to their electronic configuration close to the cuprates. For instance, LaNiO$_3$/LaAlO$_3$ superlattice has been proposed as a possible candidate. There, Ni takes a 3+ valence with d^7 configuration, and the $d_{x^2-y^2}$ orbital is lowered in energy below $d_{3z^2-r^2}$, resulting in a single electron occupation of the $d_{x^2-y^2}$ orbital [1–3]. Other materials considered as having electronic states close to the cuprates are multilayer nickelates $Ln_{n+1}Ni_nO_{2(n+1)}$ ($Ln = $ La, Nd, Pr) with no apical oxygens [4–11], where the Ni $3d_{x^2-y^2}$ band is expected to approach half filling as the number of layers n increases. In particular, the infinite-layer nickelates (LnNiO$_2$) are of special interest because Ni^{1+} valence, hence d^9 configuration, is expected if we assume Ln^{3+} and O^{2-} valence [12–18]. First-principles studies on LaNiO$_2$ have pointed out similarities as well as differences from the cuprates [19,20]. In Ref. [19], it was found that the layered structure without the apical oxygens

can favor a low-spin state when holes are doped, as in the cuprates. Also, these first-principles studies predict antiferromagnetic ordering (but with small energy gain from the paramagnetic state [20]), while no magnetism is observed experimentally [13,14]. Superconductivity, despite many years of challenge, had not been found till very recently, but superconductivity with $T_c = 9 - 15$ K has finally been discovered in a Nd$_{0.8}$Sr$_{0.2}$NiO$_2$ thin film synthesized on SrTiO$_3$ substrate [21,22]. Now we have a theoretical challenge for grasping the material's electronic structure and to resolve some important puzzles (on the mother compound being metallic without magnetism, and T_c lower than in the cuprates).

This precisely motivates the present study, where we first construct effective low-energy models for the infinite-layer nickelate to compare them with that for a high-T_c cuprate as typified by HgBa$_2$CuO$_4$. For the mother (undoped) nickelate, we shall show that a relatively small amount of holes are *self-doped* into the Ni $3d_{x^2-y^2}$ orbital due to the presence of La-originated electron pockets, which is likely to prevent the $3d_{x^2-y^2}$ band from being in a Mott insulating state. When we turn to the Sr-doped case, we shall find that the occurrence of $d_{x^2-y^2}$-wave superconductivity is suggested as in the cuprates [23], where a large intraorbital interaction (denoted as $U_{dx^2-y^2}$) within the $3d_{x^2-y^2}$ orbitals will suppress T_c due to strong renormalization effects.

The model construction is done in three steps. We start with a first-principles calculation with the local density approximation using the ECALJ package [24], from which

we obtain the model parameters in the one-body Hamiltonian in terms of the standard maximally localized Wannier functions [25,26]. We then estimate the model parameters in the many-body Hamiltonian with the constrained random-phase approximation [27], where we use the tetrahedron method [28,29] for Brillouin-zone sampling [30].

Next we explore the possibility of superconductivity and tendency toward magnetism for the obtained low-energy models with the fluctuation-exchange approximation (FLEX) [31–34], where we only consider the on-site interactions. The obtained Green's function and the pairing interaction, mediated mainly by spin fluctuations, are plugged into the linearized Eliashberg equation. We adopt the eigenvalue λ of the Eliashberg equation as a measure of superconductivity, and the spin Stoner factor α_S, given as the maximum eigenvalue of the product between the bare Coulomb interaction in the spin channel and the irreducible susceptibility $\hat{\chi}_0$ (see, e.g., Ref. [35]), as a measure of antiferromagnetism (with $\lambda = 1$ and $\alpha_S = 1$ signaling superconductivity and magnetic ordering, respectively). The eigenfunction of the Eliashberg equation having the largest λ has turned out to be $d_{x^2-y^2}$-wave pairing throughout the present study [see the inset of Fig. 3(a)]. For more details on the FLEX calculation, see the Supplemental Material [36].

Mother nickelate.—We first perform a first-principles calculation for the mother compound $LaNiO_2$ adopting the lattice parameters determined for $NdNiO_2$ in Ref. [14]. Here we consider $LaNiO_2$ instead of $NdNiO_2$ itself to avoid ambiguity for the treatment of the f-orbital bands. We show in the Supplemental Material that $LaNiO_2$ and $NdNiO_2$ in fact give essentially the same band structure (except for the f bands) if we adopt the same set of lattice parameters [36]. The obtained band structure is displayed in Fig. 1, which is similar to that obtained for $LaNiO_2$ in previous studies [19,20]. A prominent feature, as compared to the cuprates, is that, on top of the main Ni $3d_{x^2-y^2}$ band, other bands that have La $5d$ character, mixed with Ni $3d$, intersect the Fermi level. This La-originated electron pockets may be an origin of the experimentally observed metallic behavior of the resistivity at high temperatures as well as the negative Hall coefficient [17,21]. The presence of the La-originated Fermi surface also suggests that holes should be self-doped into the Ni $3d$ orbitals. We also comment on a possible effect of Nd $4f$ electrons in the Supplemental Material [36].

We now construct a low-energy model from the first-principles bands around the Fermi level. Here, we aim to construct a model that explicitly considers the Ni- and La-centered Wannier orbitals. Ni ($3d_{x^2-y^2}$, $3d_{3z^2-r^2}$, $3d_{xz}$, $3d_{yz}$), and La ($5d_{xy}$, La $5d_{3z^2-r^2}$) orbitals are known to have weights on the Fermi surface [20], where d_{z^2} is a shorthand for $d_{3z^2-r^2}$. In addition, here we opt to include the Ni $3d_{xy}$ orbital, whose band actually lies closer to the Fermi level than Ni $3d_{3z^2-r^2}$ in some portions of the Brillouin zone. In fact, we notice that the inclusion of the Ni $3d_{xy}$ is crucial for
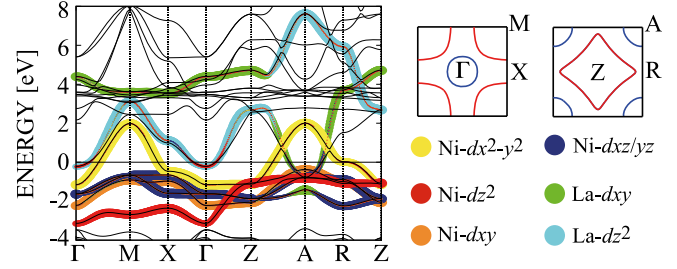

FIG. 1. First-principles band structure of $LaNiO_2$ (solid lines). The band structure of the seven-orbital model is superposed, where the Wannier-orbital weight is represented by the thickness of lines with color-coded orbital characters. Top right-hand panels display cross sections of the Fermi surface at $k_z = 0$ (left) and $k_z = \pi$ (right), where the red and blue lines depict Ni- and La-originated Fermi surfaces, respectively. See the Supplemental Material for the 3D plot of the Fermi surface [36].

stabilizing the Wannierization procedure, although it does not contribute to the Fermi surface. Another possible way to construct a model is to explicitly consider the oxygen $2p$ orbitals. We shall actually construct such models for discussions on electronic structures, while for many-body calculations such models have too many orbitals. So we mainly restrict ourselves to the above seven-orbital model, which still takes account of the oxygen orbitals through the Wannier orbitals implicitly. This simplification of incorporating the O $2p$ orbitals in the "d-only" model is often adopted in cuprate studies by introducing the concept of Zhang-Rice singlet [48], but in the present nickelate, a d-only model construction becomes even more natural due to the weaker $d − p$ hybridization than in the cuprates [19,20].

In Fig. 1, the band structure of the seven-orbital model is seen to accurately agree with the first-principles band structure. The estimated values of the on-site interactions are listed in Table I. We shall later compare these with those in the cuprates.

From charge neutrality, the total density of electrons in the seven-orbital model is 9 electrons per unit cell. The orbital-resolved density is estimated to be $n_{Nidx^2-y^2} = 0.94$, $n_{Nidz^2} = 1.83$, $n_{Nidxy} = 1.97$, $n_{Nidxz+dyz} = 3.89$, $n_{Ladz^2} = 0.12$, and $n_{Ladxy} = 0.25$. If it were not for the bands having the La character, the d^9 configuration would give $n_{Nidx^2-y^2} = 1.0$. The present result shows that about 0.06 holes per unit cell exist in the Ni $3d_{x^2-y^2}$ orbital that are self-doped from the La electron pockets.

It is thus likely that the self-doping prevents the Ni $3d_{x^2-y^2}$ band from being in a Mott insulating state. In addition, the Fermi surface of the Ni $3d_{x^2-y^2}$ band is strongly warped and its nesting is not so good that the tendency toward magnetic ordering may not be strong. In fact, previous first-principles studies predict that, although antiferromagnetism exists in $LaNiO_2$ [19,20], the energy gain from the paramagnetic state is small [20]. In the actual materials, magnetic long-range order is observed in neither

TABLE I.   The on-site interactions for the mother LaNiO$_2$ compound and $p = 0.2$ doped compound evaluated with constrained random-phase approximation. U (U') are the intraorbital (interorbital) Coulomb repulsions, and J the Hund's coupling. U for the seven-orbital model is given for Ni $3d_{x^2-y^2}$, $3d_{z^2}$ and La $5d_{xy}$, $5d_{z^2}$ orbitals, and U' and J are interactions between these orbitals. Interactions for HgBa$_2$CuO$_4$ estimated in the five-orbital model are also listed for comparison, where U' and J are those between $6s$ and $6p$ orbitals.

		LaNiO$_2$	LaNiO$_2$	($p = 0.2$)	HgBa$_2$CuO$_4$
	(eV)	Seven-orbital	Seven-orbital	Two-orbital	Five-orbital
Ni/Cu ($3d$)	$U_{dx^2-y^2}$	3.81	4.19	2.57	2.60
	U_{dz^2}	4.55	5.26	2.57	5.96
	U'	2.62	3.13	1.25	2.50
	J	0.71	0.73	0.52	0.63
La/Hg ($5d/6s, 6p$)	U_{dxy}/U_s	1.99	2.25	...	2.82
	$U_{dz^2}/U_{px,py}$	1.78	2.05	...	2.22
	U'	1.52	1.78	...	1.87
	J	0.37	0.38	...	0.22

LaNiO$_2$ nor NdNiO$_2$, which has been attributed to the Ni^{2+} centers due to excess oxygens as well as structural disorder present in the actual materials [13,14]. The present model construction suggests that the absence of the Mott insulating state together with the bad nesting may result in the absence of magnetic ordering even in an ideal, stoichiometric material. This sharply contrasts with the cuprates, where the mother compounds are Mott insulators. The mother nickelate, despite its metallicity, is not superconducting, for which we speculate should be because the electronic state of the Ni $3d_{x^2-y^2}$ band, with only a small amount of doped holes, resembles that of the heavily underdoped cuprates. The FLEX approximation cannot treat electron correlation effects in such a regime, so we will not analyze superconductivity in this regime, and leave confirmation of this picture for future studies.

Doped nickelate.—We next turn to the Sr-doped case, where superconductivity is observed experimentally [21]. Since the electron pockets in the mother compound have large La components, the rigid-band picture should be invalidated. Here we obtain the band structure using the virtual-crystal approximation (VCA), adopting the experimental lattice parameters of NdNiO$_2$ [14]. Because of technical reasons in the VCA, we use Ba instead of Sr [49]. The calculation is performed for La$_{0.8}$Ba$_{0.2}$NiO$_2$ (denoted as $p = 0.2$ hereafter), and we construct a seven-orbital model as in the mother compound. The first-principles band structure in Fig. 2(a) is seen to accurately agree with that of the seven-orbital model. The estimated interactions are listed in Table I.

Performing FLEX calculation for the seven-orbital model on a three-dimensional k mesh would be tedious, especially at low temperatures. Since the Ni $3d_{xy}$ band barely hybridizes with the other bands, ignoring this orbital in the seven-orbital model hardly affects the band structure for the remaining six orbitals, as shown in Fig. 2(b). Also, the Ni d_{xy} band is fully filled, so that we expect

that removing this band does not affect the FLEX results. We have checked this by comparing the FLEX results for the seven- and six-orbital models at $T = 0.03$ eV, where we find basically the same results with $\lambda = 0.214$, $\alpha_S = 0.926$ for the seven-orbital model and $\lambda = 0.211$, $\alpha_S = 0.926$ for the six-orbital model (see also the Supplemental Material [36]). This enables us to perform the FLEX calculation down to lower temperatures for the Ni-d_{xy}-eliminated six-orbital model, where we adopt the interaction parameters estimated for the seven-orbital model.

From the studies on the cuprates, the main player in the superconductivity in the nickelate is expected to be the Ni $3d_{x^2-y^2}$ band, which produces the main Fermi surface. To see if the orbitals that have no weight on the main Fermi surface have any effects on superconductivity or the magnetism (apart from the self-doping effect), we further construct a two-orbital model [Fig. 2(c)], where only the Ni $3d_{x^2-y^2}$ and $3d_{3z^2-r^2}$ orbitals are explicitly taken into account [50]. We can notice that the interaction parameters estimated for the two-orbital model, included in Table I, are significantly reduced from the seven-orbital counterparts. This is because the La bands are metallic, so that their
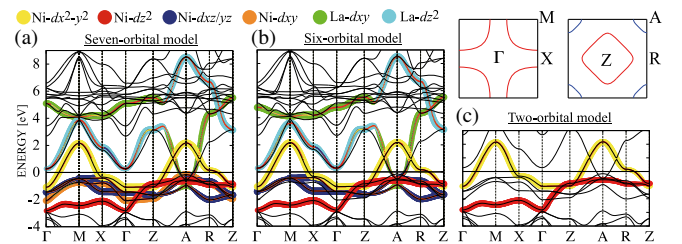

FIG. 2.   The band structure of the doped nickelate with $p = 0.2$ in (a) the seven-orbital model, (b) the six-orbital model (see text), and (c) the two-orbital model, with color-coded orbital characters, superposed with the first-principles band structure (black lines). Cross sections of the Fermi surfaces are depicted in top right as in Fig. 1.
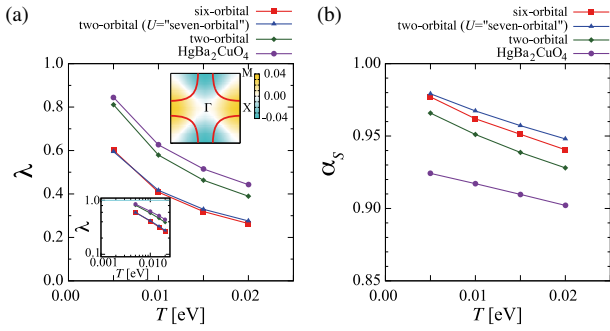
FIG. 3. Temperature dependence of the $d_{x^2-y^2}$-wave eigenvalue λ of the Eliashberg equation (a) and the Stoner factor α_S (b) for the six- and two-orbital models for $p = 0.2$. Also shown is the result for the two-orbital model with the interaction parameters taken to be as in the seven-orbital model (denoted as $U =$ "seven-orbital"). For comparison, result for $HgBa_2CuO_4$ in the five-orbital model (with the same $n_{3d_{x^2-y^2}}$ as in the $p = 0.2$ nickelate) is also shown. The insets in (a) are a log-log plot of λ versus T (bottom left), and the eigenfunction of the Eliashberg equation at $k_z = 0$ (top right; see the Supplemental Material [36] for other k_z cuts) for the six-orbital model of the nickelate ($p = 0.2$) at $T = 0.005$ eV.

screening effect, when taken into account effectively in the two-orbital model, is substantial.

To make a quantitative comparison with the cuprates, we also construct a model for $HgBa_2CuO_4$ adopting the crystal structure determined in Ref. [51]. The on-site interactions for the cuprates have been estimated in Refs. [52–54] within the $d_{x^2-y^2} - d_{z^2}$ two-orbital models, but here we construct, to make a fair comparison with the nickelate, a five-orbital model, where we explicitly take account also of the Hg $6s$, $6p_x$, and $6p_y$ orbitals, whose bands overlap with the Cu $3d_{x^2-y^2}$ band in energy (see the Supplemental Material [36]). Although this effect is not as large as that for the La $5d$ orbitals in the nickelates, it still enhances the interactions appreciably, as seen by comparing the values given in Table I with those in Ref. [52]. We have also checked that explicitly considering the t_{2g} orbitals, which do not contribute to the Fermi surface in the cuprate, has small effect on the interaction values. Then we can compare the nickelate and the cuprate, to realize that the interactions are significantly larger in the former, which should come from the smaller hybridization between the Ni and the oxygen atomic orbitals [19,20]. We shall come back to this point later.

Now we come to superconductivity. Figure 3 compares the FLEX results for λ ($d_{x^2-y^2}$-wave superconductivity) and α_S (magnetism) in the six-orbital and two-orbital models for $p = 0.2$, plotted against temperature. Since the electron pockets originating from the La orbitals are absent in the two-orbital model, we take account of the effect of self-doping there by setting the total density of electrons in such a way that $n_{Ni3d_{x^2-y^2}}$ equals the value determined from the seven-orbital model. We can immediately see that λ is

significantly reduced in the six-orbital model. This reduction of λ in the six-orbital model can come from either larger values of the interaction or the presence of the electron pockets. To identify which is the cause, we have performed another FLEX calculation for the two-orbital model adopting the same interaction values as in the seven-orbital model, as included in Fig. 3. The two-orbital model then gives results similar to those in the six-orbital model, which implies that the main origin of the reduction of λ in the six-orbital model is the large renormalization effect due to the large $U_{d_{x^2-y^2}}$, rather than the presence of the electron pockets. Conversely, we can make an observation that integrating out the La-$5d$ orbitals is inappropriate for the evaluation of the interaction parameters as far as the FLEX analysis is concerned. Namely, the two-orbital model with the on-site interaction $U_{d_{x^2-y^2}} = 2.57$ eV (in Table I) screened by La-$5d$ orbital results in an overestimation of λ. If we turn to the FLEX result for $HgBa_2CuO_4$ in the five-orbital model as included in Fig. 3 for comparison, the cuprate exhibits larger λ than the nickelate, with smaller Stoner factor. This can again be attributed to the smaller $U_{d_{x^2-y^2}}$ in the cuprate. Hence, the message here is that it is important to consider the electronic structure peculiar to the nickelate, where we have a larger $U_{d_{x^2-y^2}}$ along with a smaller bandwidth than in the cuprates, which is in turn responsible for the reduced T_c through a strong renormalization effect. We note that in Ref. [55], even larger values of $U_{d_{x^2-y^2}}$ have been obtained for a seven-orbital model of $NdNiO_2$. The origin of the discrepancy between their result and ours, as well as its effect on superconductivity, is elaborated in the Supplemental Material [36].

The larger interaction and the smaller bandwidth can be traced back to a larger level offset Δ_{dp} between $3d_{x^2-y^2}$ and oxygen $2p_{x,y}$ (atomic) orbitals for the nickelates than in the cuprates [19,20]. To evaluate Δ_{dp} quantitatively, we have also constructed models that explicitly consider the oxygen orbitals: a 23-orbital model (five Ni-$3d$, six $O - 2p$, five La-$5d$, seven La-$4f$ orbitals) for $LaNiO_2$, and a 20-orbital model (five Cu-$3d$, twelve $O - 2p$, two Hg-$6p$, and one Hg-$6s$ orbitals) for $HgBa_2CuO_4$, which gives $\Delta_{dp} = 3.7$ eV for the nickelate versus $\Delta_{dp} = 1.8$ eV for the cuprate; namely, the former is about 2 times larger than the latter (see also a recent paper [56]). For the cuprates, suppression of superconductivity due to large Δ_{dp} has been pointed out [57–59]. The reduction of T_c for large Δ_{dp} may also be viewed in terms of the strong-coupling picture, where the superexchange interaction is given as $J \propto t_{dp}^4/\Delta_{dp}^3$ with t_{dp} being the nearest-neighbor $d_{x^2-y^2} - p_{x,y}$ hopping. If we go back to the "d-only" model taking the strong-coupling viewpoint, the nearest-neighbor spin-spin interaction is estimated as $J \propto t^2/U_{d_{x^2-y^2}}$, where t is the nearest-neighbor hopping between $d_{x^2-y^2}$ orbitals. The T_c reduction for large $U_{d_{x^2-y^2}}$ and small t may also be viewed in this way.

Conversely, the present study allows us to expect that reduction of the in-plane lattice constant, which will increase the Ni $d_{x^2-y^2}$ bandwidth and reduce the interaction within the Ni $d_{x^2-y^2}$ orbital, should enhance superconductivity [60]. Hence, the smaller lattice constant in NdNiO$_2$ than in LaNiO$_2$ [13,14] may be relevant in the observation of superconductivity only in the former so far. Applying physical pressure can thus be a route toward observation of positive effects on superconductivity in the nickelate family.

Summary.—We have constructed effective models for the newly discovered nickelate superconductor. For the mother compound, a small amount of holes are self-doped into the Ni $3d_{x^2-y^2}$ orbital due to the presence of electron pockets. These electron pockets may have relevance to the metallic behavior observed experimentally [17,21], while the electronic state of the $3d_{x^2-y^2}$ band with a hole self-doping may be close to that of the heavily underdoped cuprates [23] with no magnetism or superconductivity. For the Sr-doped nickelate, the FLEX study for the six-orbital model that incorporates La orbitals indicates that $d_{x^2-y^2}$-wave superconductivity is suggested to arise as in the cuprates, but that a larger interaction within the Ni $d_{x^2-y^2}$ orbital along with a narrower bandwidth than in the cuprates results in a lower T_c due to the strong self-energy renormalization effect. We may also conclude that, if the present d-only model captures the essence of the nickelate superconductivity, this will imply that the strength of the $d - p$ hybridization (whether the mother insulator is in the Mott-Hubbard or the charge-transfer regime [61]) does not qualitatively affect the occurrence of superconductivity. Important future problems include exploration of related materials with different elements and/or compositions, which may result in a possible enhancement of T_c.

---

[*]sakakibara.tottori.u@gmail.com

[1] J. Chaloupka and G. Khaliullin, Phys. Rev. Lett. **100**, 016404 (2008).

[2] P. Hansmann, X. Yang, A. Toschi, G. Khaliullin, O. K. Andersen, and K. Held, Phys. Rev. Lett. **103**, 016401 (2009).

[3] M. J. Han, X. Wang, C. A. Marianetti, and A. J. Millis, Phys. Rev. Lett. **107**, 206804 (2011).

[4] J. Zhang, A. S. Botana, J. W. Freeland, D. Phelan, H. Zheng, V. Pardo, M. R. Norman, and J. F. Mitchell, Nat. Phys. **13**, 864 (2017).

[5] V. Pardo and W. E. Pickett, Phys. Rev. Lett. **105**, 266402 (2010).

[6] J.-G. Cheng, J.-S. Zhou, J. B. Goodenough, H. D. Zhou, K. Matsubayashi, Y. Uwatoko, P. P. Kong, C. Q. Jin, W. G. Yang, and G. Y. Shen, Phys. Rev. Lett. **108**, 236403 (2012).

[7] R. Retoux, J. Rodriguez-Carvajal, and P. Lacorre, J. Solid State Chem. **140**, 307 (1998).

[8] N. ApRoberts-Warren, A. P. Dioguardi, V. V. Poltavets, M. Greenblatt, P. Klavins, and N. J. Curro, Phys. Rev. B **83**, 014402 (2011).

[9] V. V. Poltavets, K. A. Lokshin, A. H. Nevidomskyy, M. Croft, T. A. Tyson, J. Hadermann, G. Van Tendeloo, T. Egami, G. Kotliar, N. ApRoberts-Warren, A. P. Dioguardi, N. J. Curro, and M. Greenblatt, Phys. Rev. Lett. **104**, 206403 (2010).

[10] V. V. Poltavets, K. A. Lokshin, S. Dikmen, M. Croft, T. Egami, and M. Greenblatt, J. Am. Chem. Soc. **128**, 9050 (2006).

[11] O. O. Bernal, D. E. MacLaughlin, G. D. Morris, P.-C. Ho, L. Shu, C. Tan, J. Zhang, Z. Ding, K. Huang, and V. V. Poltavets, Phys. Rev. B **100**, 125142 (2019).

[12] M. Crespin, P. Levitz, and L. Gatineau, J. Chem. Soc. Faraday Trans. **79**, 1181 (1983).

[13] M. A. Hayward, M. A. Green, M. J. Rosseinsky, and J. Sloan, J. Am. Chem. Soc. **121**, 8843 (1999).

[14] M. Hayward and M. Rosseinsky, Solid State Sci. **5**, 839 (2003).

[15] M. Kawai, S. Inoue, M. Mizumaki, N. Kawamura, N. Ichikawa, and Y. Shimakawa, Appl. Phys. Lett. **94**, 082102 (2009).

[16] D. Kaneko, K. Yamagishi, A. Tsukada, T. Manabe, and M. Naito, Physica (Amsterdam) **469C**, 936 (2009).

[17] A. Ikeda, Y. Krockenberger, H. Irie, M. Naito, and H. Yamamoto, Appl. Phys. Express **9**, 061101 (2016).

[18] T. Onozuka, A. Chikamatsu, T. Katayama, T. Fukumura, and T. Hasegawa, Dalton Trans. **45**, 12114 (2016).

[19] V. I. Anisimov, D. Bukhvalov, and T. M. Rice, Phys. Rev. B **59**, 7901 (1999).

[20] K.-W. Lee and W. E. Pickett, Phys. Rev. B **70**, 165109 (2004).

[21] D. Li, K. Lee, B. Y. Wang, M. Osada, S. Crossley, H. R. Lee, Y. Cui, Y. Hikita, and H. Y. Hwang, Nature (London) **572**, 624 (2019).

[22] G. A. Sawatzky, Nature (London) **572**, 592 (2019), an associate article of Ref. [21].

[23] B. Keimer, S. A. Kivelson, M. R. Norman, S. Uchida, and J. Zaanen, Nature (London) **518**, 179 (2015).

[24] A first-principles electronic-structure suite based on the PMT method, ECALJ package, https://github.com/tkotani/ecalj.

[25] N. Marzari and D. Vanderbilt, Phys. Rev. B **56**, 12847 (1997).

[26] I. Souza, N. Marzari, and D. Vanderbilt, Phys. Rev. B **65**, 035109 (2001).

[27] F. Aryasetiawan, M. Imada, A. Georges, G. Kotliar, S. Biermann, and A. I. Lichtenstein, Phys. Rev. B **70,** 195104 (2004).

[28] T. Kotani, M. van Schilfgaarde, and S. V. Faleev, Phys. Rev. B **76,** 165106 (2007).

[29] T. Kotani, J. Phys. Soc. Jpn. **83,** 094711 (2014).

[30] We take $12 \times 12 \times 12(12 \times 12 \times 6)$ or $10 \times 10 \times 10$ $(8 \times 8 \times 4)$ k points in the local density approximation calculation or in the Wannierization procedure for $LaNiO_2(HgBa_2CuO_4)$, respectively.

[31] N. E. Bickers, D. J. Scalapino, and S. R. White, Phys. Rev. Lett. **62,** 961 (1989).

[32] N. E. Bickers and S. R. White, Phys. Rev. B **43,** 8044 (1991).

[33] A. I. Lichtenstein and M. I. Katsnelson, Phys. Rev. B **57,** 6884 (1998).

[34] H. Ikeda, R. Arita, and J. Kuneš, Phys. Rev. B **81,** 054502 (2010).

[35] H. Sakakibara, H. Usui, K. Kuroki, R. Arita, and H. Aoki, Phys. Rev. B **85,** 064501 (2012).

[36] See Supplemental Material at http://link.aps.org/supplemental/10.1103/PhysRevLett.125.077003 for details, which includes Refs. [37–47].

[37] G. Kresse and J. Hafner, Phys. Rev. B **47,** 558 (1993).

[38] G. Kresse and J. Hafner, Phys. Rev. B **49,** 14251 (1994).

[39] G. Kresse and J. Furthmüller, Phys. Rev. B **54,** 11169 (1996).

[40] G. Kresse and J. Furthmüller, Comput. Mater. Sci. **6,** 15 (1996).

[41] E. Şaşıoğlu, C. Friedrich, and S. Blügel, Phys. Rev. B **83,** 121101(R) (2011).

[42] P. Giannozzi et al., J. Phys. Condens. Matter **29,** 465901 (2017).

[43] J. P. Perdew, K. Burke, and M. Ernzerhof, Phys. Rev. Lett. **77,** 3865 (1996).

[44] D. R. Hamann, Phys. Rev. B **88,** 085117 (2013).

[45] M. van Setten, M. Giantomassi, E. Bousquet, M. Verstraete, D. Hamann, X. Gonze, and G.-M. Rignanese, Comput. Phys. Commun. **226,** 39 (2018).

[46] RESPACK, https://sites.google.com/view/kazuma7k6r.

[47] T. Kotani, H. Kino, and H. Akai, J. Phys. Soc. Jpn. **84,** 034702 (2015).

[48] F. C. Zhang and T. M. Rice, Phys. Rev. B **37,** 3759 (1988).

[49] In the ECALJ code, VCA can be performed only for elements adjacent to each other in the periodic table. We have checked, with the VASP code, that the band structure is not strongly affected when Ba is used in place of Sr (see Supplemental Material [36]).

[50] H. Sakakibara, H. Usui, K. Kuroki, R. Arita, and H. Aoki, Phys. Rev. Lett. **105,** 057003 (2010).

[51] J. Wagner, P. Radaelli, D. Hinks, J. Jorgensen, J. Mitchell, B. Dabrowski, G. Knapp, and M. Beno, Physica (Amsterdam) **210C,** 447 (1993).

[52] S. W. Jang, H. Sakakibara, H. Kino, T. Kotani, K. Kuroki, and M. J. Han, Sci. Rep. **6,** 33397 (2016).

[53] H. Sakakibara, S. W. Jang, H. Kino, M. J. Han, K. Kuroki, and T. Kotani, J. Phys. Soc. Jpn. **86,** 044714 (2017).

[54] H. Sakakibara and T. Kotani, Phys. Rev. B **99,** 195141 (2019).

[55] Y. Nomura, M. Hirayama, T. Tadano, Y. Yoshimoto, K. Nakamura, and R. Arita, Phys. Rev. B **100,** 205138 (2019).

[56] A. S. Botana and M. R. Norman, Phys. Rev. X **10,** 011024 (2020).

[57] S. Shinkai, H. Ikeda, and K. Yamada, J. Phys. Soc. Jpn. **75,** 104712 (2006).

[58] C. Weber, C. Yee, K. Haule, and G. Kotliar, Europhys. Lett. **100,** 37001 (2012).

[59] C. Weber, K. Haule, and G. Kotliar, Phys. Rev. B **82,** 125107 (2010).

[60] One may consider that the reduction of the lattice constant would affect phonons, which in turn may affect superconductivity. However, it has been revealed by Nomura et al. in Ref. [55] that the electron-phonon interaction is weak in the present nickelate.

[61] J. Zaanen, G. A. Sawatzky, and J. W. Allen, Phys. Rev. Lett. **55,** 418 (1985).